Available online at www.sciencedirect.com
SCIENCE DIRECT
Surface Science xxx (2006) xxx–xxx
SURFACE SCIENCE
www.elsevier.com/locate/susc

# Diffusion processes in seeded and unseeded SBT thin films with varied stoichiometry

G. González Aguilar [a], A. Wu [a], M.A. Reis [b], A.R. Ramos [b], I.M. Miranda Salvado [a], E. Alves [b], M.E.V. Costa [a,*]

[a] CICECO, Depto. Eng. Cerâmica e do Vidro, Universidade de Aveiro, Campus de Santiago, Aveiro 3810-193, Portugal
[b] Instituto Tecnológico e Nuclear, Estrada Nacional no 10, P-2685 Sacavém, Portugal

Received 4 November 2005; accepted for publication 31 January 2006

**Abstract**

$SrBi_2Ta_2O_9$ (SBT) is a bismuth layered perovskite (BLP) with interesting ferroelectric properties for memories applications. The previous study on the synthesis of seeded and unseeded SBT thin films by the authors [G. González Aguilar, M.E.V. Costa, I.M. Miranda Salvado, J. Eur. Ceram. Soc. 25 (2005) 2331] has shown an increase of the crystallinity of the films and an improvement of the thin film ferroelectric properties when using SBT seeds. However, the detailed role of the seeds as an improver of the thin film properties has not been investigated so far. In the present work we study the role of the seeds, particularly with respect to the reactions between film and (bottom) underlying platinum electrode. The comparison of the results obtained by characterizing the seeded and unseeded thin films via Rutherford backscattering (RBS) and particle induced X-ray emission (PIXE) techniques reveals an effective modification of the substrate–thin film interface by the presence of the seeds. Moreover, the evaluation of the thin film ferroelectric properties by atomic force microscopy (AFM) shows an improvement of the local piezoelectric hysteresis loops by the seeds. These seeding effects as well as those observed in non-stoichiometric SBT thin films with different bismuth contents are used to discuss the barrier-like role of the SBT seeds against reactions between film and the platinum electrode and its contribution to the improvement of the thin film properties.


*Keywords:* Surface chemical reaction; Surface diffusion; Rutherford backscattering spectrometry (RBS); Thin film structures; Metal–oxide interfaces; Ferroelectric films

## 1. Introduction

The intensive research focused on $SrBi_2Ta_2O_9$ (SBT) and $SrBi_2Nb_2O_9$ (SBN) thin films revealed these ferroelectric compounds to be competitive candidates for non-volatile ferroelectric random access memories (NV-FRAMs) applications. The structure of these bismuth layered perovskites (BLP) also known as Aurivillius oxides consists of $Bi_2O_2^{2+}$ layers alternating with strontium tantalate ($SrTa_2O_7^{2-}$) (or strontium niobate ($SrNb_2O_7^{2-}$)) perovskite units, respectively. SBT and SBN present several advantages over other ferroelectric compounds, namely $Pb(Zr_{1-x}Ti_x)O_3$, which include a fatigue-free behavior, good retention properties and low leakage currents [2]. In addition the toxicity issues associated to BLP are of lower concern as they are lead free compounds.

As a consequence of such appealing features, great attention has been focused on the improvement of the less attractive characteristics of these materials. For example, several doping studies were reported for improving the value of the remnant polarization (Pr) [3,4], for reducing the perovskite crystallization temperature [5,6] and even for recovering the properties of the films after fatigue [7]. A different approach based on a seeding procedure, either using seeds like SBT seeds [1], Bi and Bi/Ta seeds [8] or $Bi_2SiO_5$ seeds [5], or using a seeding layer of $Bi_4Ti_3O_{12}$ [8] has also been successful in improving the thin film characteristics.

* Corresponding author. Tel.: +351 234 370 354; fax: +351 234 425 300.
*E-mail address:* elisabete@cv.ua.pt (M.E.V. Costa).

0039-6028/$ - see front matter © 2006 Elsevier B.V. All rights reserved.
doi:10.1016/j.susc.2006.01.051

The role of SBT seeds in the crystallization of SBT thin films has been described [9] as promoting the perovskite phase formation by two mechanisms: (1) lowering the activation energy for Aurivillius oxide nucleation and crystal growth, hence favoring its growth kinetics with respect to other coexisting phases such as pyrochlore and (2) allowing diffusion of SBT film bismuth ions driven by bismuth concentration gradients which contribute to the transformation of the existing Bi-deficient pyrochlore seeds into perovskite phase.

Due to the high structural anisotropy of BLP, which have spontaneous polarization vector lying perpendicular to *c*-axis, the crystallographic orientation of the film with respect to the substrate has been also of great concern for optimizing its electrical properties. Some studies have shown that the type and orientation of the interface material between the substrate or seeding layer and the thin film may have a strong effect on the growth of the film [9–13]. However, when using a seeding layer, the contribution of the seeds for the interface chemistry has not been investigated yet.

The objective of the present work is to get deeper insight into the role of the seeds, in particular regarding the bottom electrode–thin film interface phenomena. For this purpose the results obtained via Rutherford backscattering (RBS) and particle induced X-ray emission (PIXE) on seeded and unseeded SBT thin films with varied stoichiometry are used for evaluating the effects of the SBT seeds on the inter-diffusion between the film and underlying electrode constituents. Combining RBS and PIXE results with ferroelectric and atomic force microscopy (AFM) characterization results, a discussion of the effect of stoichiometry deviation and of the seeding procedure in the thin film properties is presented.

## 2. Experimental

Seeded and unseeded SBT films were prepared by spin-coating organic solutions of the required cations on Si/SiO2/Ti/Pt substrates followed by drying at 180 °C. After several spinning-drying cycles a heat treatment at 720 °C for 30 min was done. The metallorganic solution was prepared by a modified sol–gel procedure: briefly, bismuth acetate (Aldrich, S. Louis), strontium acetate (ABCR, Karlsruhe) and tantalum ethoxide (Fluka, Buchs) were dissolved in an organic solvent mixture (1:1) of toluene (Riedel-de Haën, Seelze) and acrylic acid (Fluka, Buchs), under controlled atmosphere. Different cation proportions were selected so as to obtain nominal stoichiometric and non-stoichiometric (Bi-deficient) compositions. For seeded films, seeds were previously deposited by spin-coating on the substrate. The details of the experimental procedures are published elsewhere [1]. Table 1 identifies the samples used in the current work. The film crystalline structure was analyzed by grazing incidence X-ray diffraction (Philips X'Pert MPD X-ray diffractometer with CuK$\alpha$ radiation), which confirmed the crystalline perovskite structure of all the prepared films without any second phases. The average thickness of the obtained thin films was around 500 nm as evaluated by scanning electron microscopy measurements.

Table 1
Identification of the studied thin films

| Thin film stoichiometry | Sample code* | Heat treatment temperature (°C) | Seeds |
|---|---|---|---|
| $SrBi_{1.5}Ta_2O_9$ | U72-1.5 | 720 | No |
| $SrBi_{1.7}Ta_2O_9$ | U72-1.7 | 720 | No |
| $SrBi_{1.9}Ta_2O_9$ | U72-1.9 | 720 | No |
| $SrBi_{1.9}Ta_2O_9$ | S72-1.9 | 720 | Yes |
| $SrBi_2Ta_2O_9$ | U72-2.0 | 720 | No |
| $SrBi_2Ta_2O_9$ | S72-2.0 | 720 | Yes |

* S stands for seeded; U stands for unseeded; 7× indicates heat treated at $7 \times 0$ °C; *y.z* stands for Bi stoichiometry ($Bi_{y.z}$).

Rutherford backscattering spectrometry (RBS) and particle induced X-ray emission (PIXE) analyses were performed using a 2.5 MV Van de Graaff Accelerator. RBS spectra were obtained with 2 Schottky barrier detectors placed in IBM geometry at 140° and 180° scattering angles, with resolutions of 15 and 25 keV, respectively, using a 2.250 and a 2 MeV $He^+$ beam. Analyses were performed with samples tilted at 0°, 20° or 30° (angle between beam direction and sample normal). PIXE measurements were performed with a 2.15 MeV $H^+$ beam and the X-rays were detected with a Gresham Scirus detector with 155 eV energy resolution placed at 110° to beam direction and at a distance of 25 mm from the samples. The PIXE spectra were analysed using the AXIL [10] and DATTPIXE codes [11] and RBS spectra with the NDF code [12].

The ferroelectric properties were measured with a TFA analyzer (AIXACCT, Model: TFA-LI). The film surface topography was analyzed by atomic force microscopy (AFM) using commercial AFM equipment (Multimode, Nanoscope IIIA, Digital Instruments). A conductive Pt-coated Si tip-cantilever (NSG01/Pt, NT-MDT Co., Russia) system was used as a top electrode and for vibration detection. Local piezoelectric hysteresis loops were performed via piezoresponse mode (PFM) that relies on a local piezoelectric effect exhibited by film's surface.

## 3. Results and discussion

In the RBS spectra, the Sr, Bi and Ta backscattering signals appear convoluted, thus impairing a direct determination of the Ta, Sr and Bi concentrations from these spectra. To overcome this inconvenient the samples were analyzed by PIXE. The results obtained showed that, with the exception of sample U72-1.5, the composition of the films does not deviate significantly from the nominal composition. As regards the nominal non-stoichiometric films, which were prepared with specific Bi deficiencies (Table 1), the combined PIXE–RBS results confirmed them to be non-stoichiometric, though with slight variations from the nominal composition. Selected results are shown in Table 2.

The Ta/Sr and Bi/Sr ratios determined by PIXE were used for simulating the experimental RBS spectra, thus

Table 2
Combined PIXE/RBS composition results

| Sample | Nominal composition | | | Simulation results | | | Ta-normalized results | | |
|---|---|---|---|---|---|---|---|---|---|
| | Sr | Bi | Ta | Sr | Bi/Sr | Ta/Sr | Sr | Bi | Ta |
| U72-1.5 | 1.00 | 1.50 | 2.00 | 1.00 | 1.7 | 2.3 | 0.9 | 1.5 | 2.0 |
| U72-1.7 | 1.00 | 1.70 | 2.00 | 1.00 | 1.7 | 2.00 | 1.0 | 1.7 | 2.0 |
| U72-1.9 | 1.00 | 1.90 | 2.00 | 1.00 | 1.9 | 2.2 | 0.9 | 1.8 | 2.0 |
| S72-1.9 | 1.00 | 1.90 | 2.00 | 1.00 | 1.9 | 2.0 | 1.0 | 1.9 | 2.0 |
| U72-2.0 | 1.00 | 2.00 | 2.00 | 1.00 | 1.9 | 2.0 | 1.0 | 2.0 | 2.0 |
| S72-2.0 | 1.00 | 2.00 | 2.00 | 1.00 | 2.0 | 1.9 | 1.0 | 2.1 | 2.0 |

allowing the determination of the depth concentration profiles corresponding to the different elements to be evaluated (Fig. 1). In the case of sample S72-1.9, Fig. 1d, some gold is observed by RBS. This is due to the fact that the analyzing beam on this sample partly hit a deposited gold contact. This fact does not influence the concentration values obtained in Table 2 or the following discussion.

Comparing Fig. 1c–f it is possible to see that sharper interfaces between SBT film and platinum electrode are observed in seeded films (Fig. 1d and f) when compared to their unseeded counterparts (Fig. 1c and e). These last ones display a stepped interface denoting some intermixing of Pt and film components, which may result from the inter-diffusion of underlying Pt electrode and the SBT thin film elements, due to a solid state reaction amongst them, and/or being due to interface roughness. As an example, Fig. 2 shows the RBS spectra of samples U72-2.0 and S72-2.0 (concentration profiles in Fig. 1e and f). A clear difference in the interface region is observed. The concentration profiles shown in Fig. 1 also demonstrate that, when increasing the bismuth content in unseeded films, interface changes become more evident, as evidenced by the total amount of Pt in the Pt/film interface (compare Fig. 1a, b and e). The only exception is sample U72-1.9. This probably reflects small and uncontrollable differences in the thin films processing conditions such as different humidity/pressure conditions that could influence side reactions.

The chemistry of interfaces and surfaces usually requires sophisticated and sometimes indirect methods to establish the reactions occurring during a given process. More often, these methods cannot afford each individual reaction step contributing for the complex process under study. In these cases a post-mortem analysis of the suspected mechanism is the only source of knowledge. In order to frame the discussion of the different diffusion phenomena envisaged for SBT/Si/$SiO_2$/Ti/Pt interface during the thermal processing of SBT thin film on a platinum surface, several reaction possibilities involving the metallic atoms are reviewed as follows:

(i) Decomposition of precursor cation carboxilates under heating, leading to their respective oxides as described by Eqs. (1)–(3):

$$Ta(OOCR)_5 + nO_2 \rightarrow TaO_y + mCO_2 \quad (1)$$

$$Sr(OOCR)_2 + nO_2 \rightarrow SrO_v + mCO_2 \quad (2)$$

$$Bi(OOCR)_3 + nO_2 \rightarrow BiO_x + mCO_2 \quad (3)$$

(ii) Combination reaction of the oxides, Eq. (4):

$$2BiO_x + 2TaO_y + SrO_v \rightarrow SrBi_2Ta_2O_{(2x+2y+v)} \quad (4)$$

This equation is naturally affected by the uptake of elements by other competing parallel reactions.

(iii) Bismuth reduction to metallic bismuth, Eq. (5):

$$Bi(OOCR)_3 \rightarrow Bi + nC + mCO_2 \quad (5)$$

This reaction may take place when oxygen is the limiting species [13], either due to a low oxygen pressure or due to the presence of long hydrocarbon chains providing high concentration of carbon and hydrogen and/or to other coexisting reducing reagents [14,15]. When the oxygen concentration is sufficiently high, the above reduction reaction has little chance to occur, as bismuth is highly reactive towards oxidation [16]. In fact metallic bismuth has been found in BLP compounds processed at high temperature but only under serious reducing conditions [14].

(iv) Interface reaction between Bi and Pt, Eqs. (6) and (7):

$$Pt + Bi \rightarrow PtBi \quad (6)$$

$$Pt + 2Bi \rightarrow PtBi_2 \quad (7)$$

The synthesis of Pt–Bi alloys (Eqs. (6) and (7)) has been achieved in an oxygen-free atmosphere at 800 °C for 48 h in a sealed tube (also to avoid bismuth evaporation), followed by an annealing at 650 °C for 24 h [17]. Such prolonged heating process indicates these reactions to be most unlikely to occur during the short annealing times (usually 1–2 h) used in SBT synthesis. Even so, assuming that temporary conditions including high local concentration of metallic bismuth and low oxygen concentration may allow the synthesis of such intermetallic compounds, then some limited diffusion of Bi and Pt species should be considered at the film–electrode interface [18].

(v) Interface reaction between $BiO_x$ and Pt, Eq. (8):

$$Pt + BiO_x \rightarrow PtBiO_x \quad (8)$$

This type of interaction between platinum and bismuth oxide was already detected by RBS studies during the synthesis of SBT which also showed the presence of $PtBi_x$ [19]. Considering the low melting point of bismuth (271 °C) and that of bismuth oxide (820 °C), the heat treatment of SBT films at temperatures ranging from 700 up to 850 °C is prone to diffusion phenomena, either of metallic or of

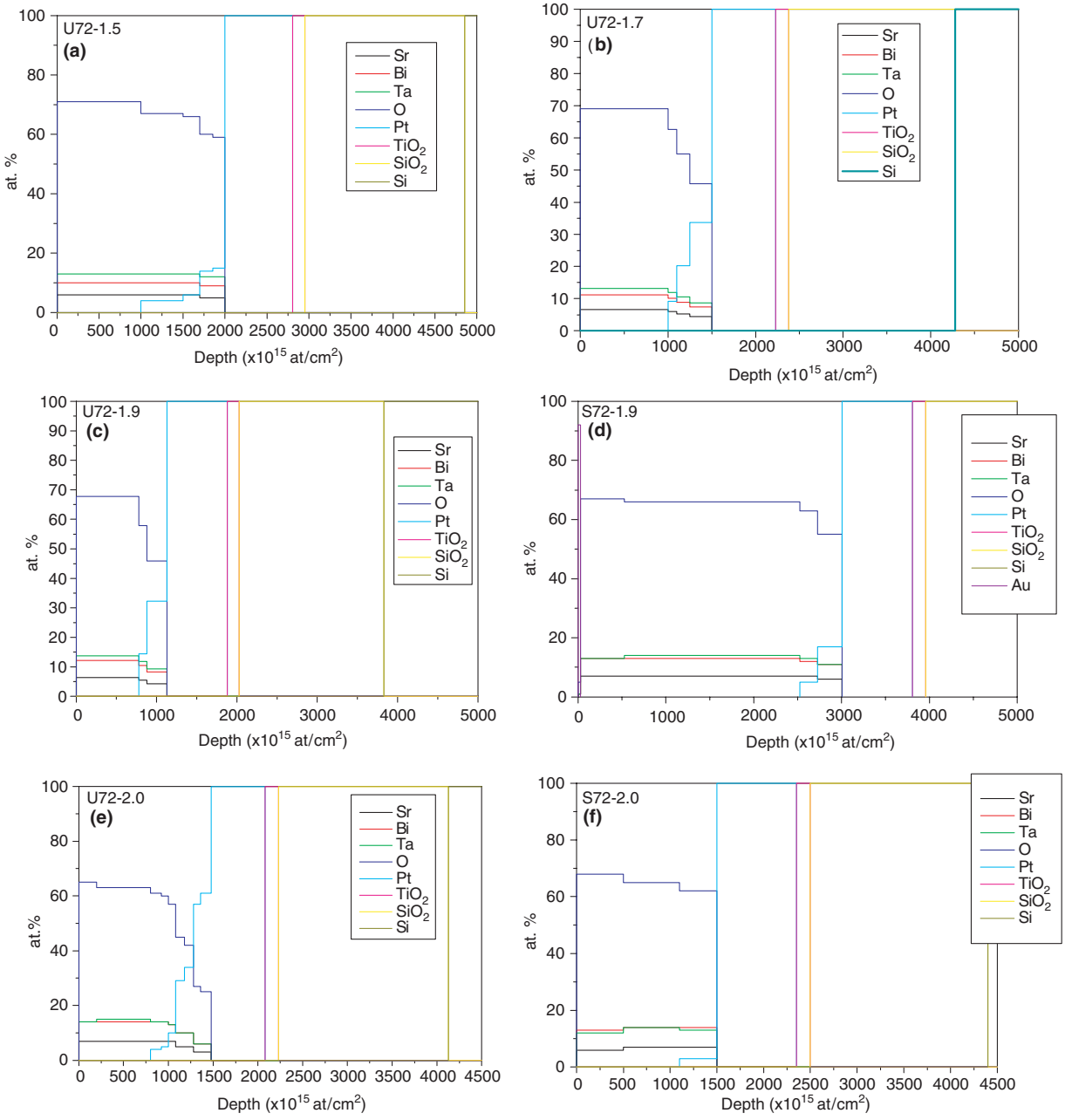


Fig. 1. Simulated concentration profiles of SBT thin films based on PIXE/RBS analysis results.

cationic species. So, reactions (6)–(8) may occur in a rather significant extension when SBT synthesis conditions include relatively high concentrations of Bi.

(vi) Interface reaction between Ta and/or Sr oxides and Pt, Eqs. (9) and (10):

$$Pt + SrO_x \rightarrow PtSrO_x \quad (9)$$

$$Pt + TaO_x \rightarrow PtTaO_x \quad (10)$$

The diffusion process of Sr towards the platinum substrate was theoretically studied [20] to determine the most energetically favorable growth of Pt on a $SrTiO_3$ surface, a moderate inter-diffusion of these elements being predicted. Tantalum was experimentally observed to be involved in intermetallic association with Pt but only when using an inert atmosphere [21], because under the used working temperature (720 °C) the presence of oxygen readily oxidizes Ta. At that temperature the above mentioned diffusion reactions may occur at a much slower rate than the bismuth platinum interaction described by Eqs. (6) and (7).

The results presented in Table 2 and Fig. 1 show that the highly non-stoichiometric sample U72-1.5 does not exhibit any obvious depletion of Bi relatively to its nominal composition. The slight Ta enhancement seen in this case on the PIXE composition may be just an artifact due to an underlying Pt electrode complex interface. The RBS spec-

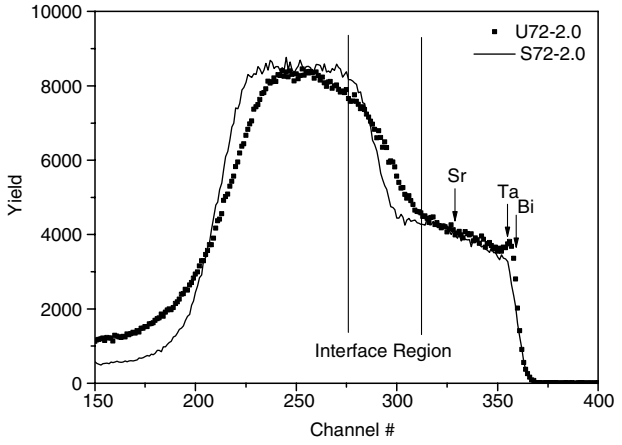


Fig. 2. RBS spectra of samples U72-2.0 and S72-2.0. RBS spectra acquired using a 2.0 MeV $He^{+}$ beam, with the 140° scattering angle detector and a tilt angle of 30°.

tra fitting are being compatible with this interpretation. In view of the Bi deficiencies of this composition and bearing in mind the competition among the different reactions for bismuth consumption (Eqs. (4)–(8)), it is thought that its concentration is insufficient for allowing some of the reactions leading to interface Bi compounds to proceed.

However, when increasing Bi content in unseeded films, it is generally seen that an interface containing Pt, Bi, Sr, Ta and high contents of oxygen is formed (Fig. 1), hence indicating reaction products of Pt with SBT film components to be present. Accordingly the interface sharpness is now replaced by a stepped Pt concentration profile denoting significant Pt/film intermixing, which could suggest some interface reaction.

The introduction of seeds modifies significantly the electrode/film interface, contributing to restore the interface sharpness, as shown in Fig. 1 and Table 2 (compare samples U72-1.9; S72-1.9; U72-2.0 and S72-2.0). It may thus be concluded that seeded films do not afford suitable conditions for interface reactions as their unseeded counterparts do. As mentioned above, a role has been proposed for the seeds by Jung et al. [9] in the framework of perovskite crystallization. However the present results address a new perspective for the seeds role as a conditioner of the electrode/film interface phenomena.

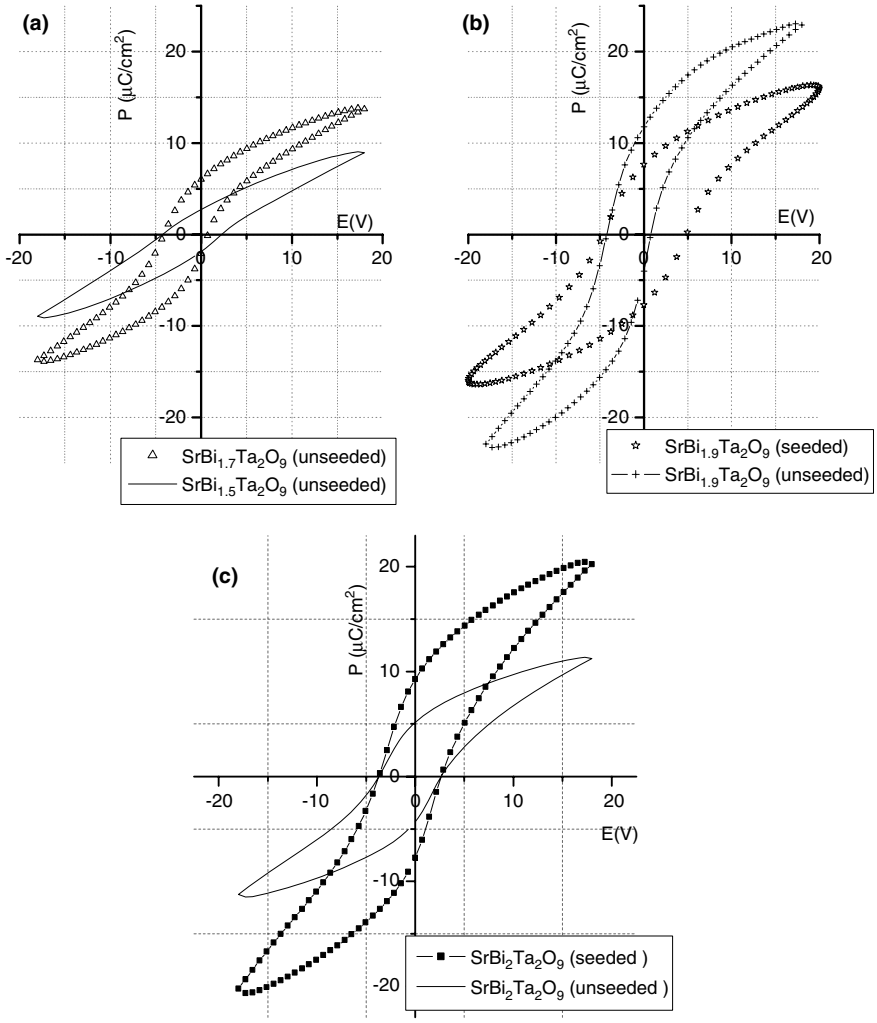


Fig. 3. Hysteresis loops of seeded and unseeded SBT films prepared with different stoichiometries at 720 °C.

As described, the deposition of SBT seeds was followed by a heat treatment at 180 °C. This treatment supplies enough energy for the establishment of Van der Waals interactions between the platinum layer and the seeds. It is thought that these (weakly) bonded seeds act as a physical barrier against the diffusion of the constituents of the deposited solution towards the platinum layer. Moreover, once the perovskite phase is crystallized, the (chemical) interaction of platinum with the already formed SBT phase would require the following reaction to occur:

$$\mathrm{SBT} \rightarrow \mathrm{BiO}_x + \mathrm{bTaO}_y + c\mathrm{SrO} \quad (11)$$

or

$$\mathrm{SBT} \rightarrow \mathrm{BiO}_x + \mathrm{SrTa_2O_6} \quad (12)$$

These decomposition reactions are unlikely to occur due to the high stability of the perovskite network: the activation energy of reaction (11) was calculated to be 264 kJ/mol [9] so high temperatures are needed to break out the SBT network and reverse the reaction. Consequently, in the presence of seeds, reactions (6)–(8) will occur in a reduced extension, probably limited to sites where diffusion processes may proceed easily like possible cracks or pores of the thin film structure.

Fig. 3 compares the ferroelectric behavior of some of the prepared samples. The enhancement of the ferroelectric behavior as the thin film Bi content increases is clearly observed though the hysteresis loops of the non-stoichiometric films are strongly displaced (or shifted) along the

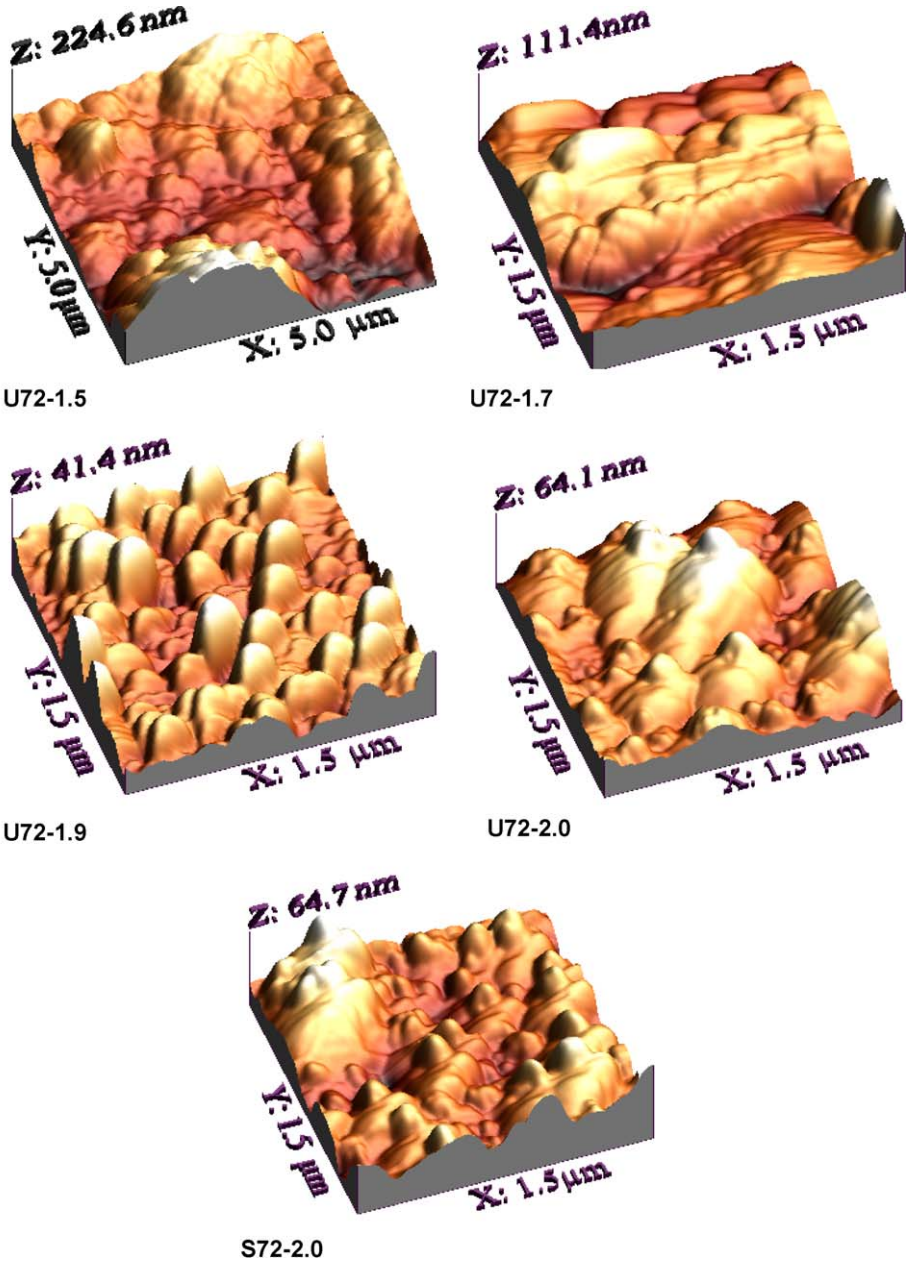


Fig. 4. AFM analysis of the surface morphology of seeded and unseeded SBT films with different stoichiometry.

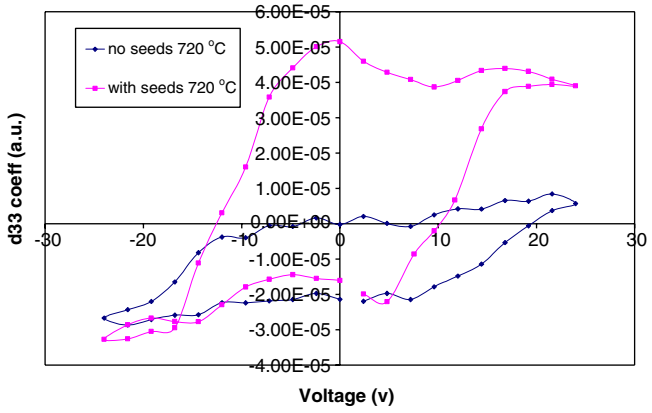


Fig. 5. Local piezoelectric hysteresis loops acquired in SBT grains of seeded and unseeded stoichiometric films.

*P*-axis (see Fig. 3a and b). This may cause space charge at the ferroelectric-electrode interface [22,23]. Another important feature revealed by the figure is that the presence of seeds improves significantly the hysteresis loops of the thin films: the seeded samples of the $SrBi_{1.9}Ta_2O_9$ and $SrBi_2Ta_2O_9$ compositions show higher remnant polarization than their corresponding unseeded ones. This finding suggests that the thin film/Pt electrode interface is of great relevance for the ferroelectric behavior of the SBT thin film.

The AFM images (Fig. 4) show more irregular structures for the non-stoichiometric and unseeded films when compared to their seeded counterparts. In these films the grain sizes are not homogeneously distributed, with big grains around 300 nm and some small grains around 10–20 nm while stoichiometric and seeded films show a relatively regular grain size distribution and a homogeneous surface microstructure. The rms (root mean square) roughness of the films was seen to be in the range of 5–17 nm without apparent correlation with the composition or the presence of seeds.

Local piezoelectric hysteresis loops of single grain in unseeded and seeded samples were measured by PFM. It was observed that seeded film always show higher remnant $d_{33}$ coefficient values than that of unseeded films. This behavior is illustrated in Fig. 5 where the obtained typical local piezoelectric hysteresis loops for the seeded and unseeded stoichiometric film is presented. Consistent with the above mentioned results, the inhibition of the reaction between films/Pt-layer by seeds maintained the film composition within its stoichiometry and therefore superior electrical properties in microscopic region were revealed.

## 4. Conclusions

The films synthesized without seeds show the formation of an interface of variable content and/or shape. The use of seeds as revealed by the present results contributes to a higher stability of the film and electrode constituents thus suggesting an inhibition effect of the seeds regarding interface reactions. Moreover, the seeds also benefit the homogeneity of the thin film surface microstructure as well as the ferroelectric properties: the macroscopic *P–E* hysteresis loops and the local piezoloops showed that seeded films present higher remnant polarization values and higher average remanent $d_{33}$ than their unseeded counterparts. The barrier-like role of the seeds while preventing the inter-diffusion between films/Pt-layer helps preserving the thin film composition and therefore enhanced electrical properties are observed.

## Acknowledgements

GGA thanks the Portuguese Fundação para a Ciencia e a Tecnologia (FCT) for a PhD grant.

## References

[1] G. González Aguilar, M.E.V. Costa, I.M. Miranda Salvado, J. Eur. Ceram. Soc. 25 (2005) 2331.
[2] Y.-B. Park, J.-K. Lee, H.-J. Jung, J.-W. Park, J. Mater. Res. 14 (1999) 2986.
[3] J. Zhu, X. Zhang, Y. Zhu, S.B. Desu, J. Appl. Phys. 83 (1998) 1610.
[4] Y. Zhong, G. Hu, T.-A. Tang, Jpn. J. Appl. Phys. 42 (2003) 7424.
[5] X. Wang, S. Yamamoto, H. Ishiwara, Jpn. J. Appl. Phys. 41 (2002) L1492.
[6] S.-Y. Chen, V.-Ch. Lee, J. Appl. Phys. 87 (2000) 3050.
[7] T. Osaka, T. Yoshie, T. Hoshika, I. Koiwa, Y. Sawada, A. Hashimoto, Jpn. J. Appl. Phys. 39 (2000) 5476.
[8] G.D. Hu, J.B. Xu, I.H. Wilson, W.Y. Cheung, N. Ke, S.P. Wong, Appl. Phys. Lett. 74 (1999) 3711.
[9] S.-Y. Jung, S.-J. Hwang, Y.-M. Sung, J. Mater. Res. 18 (2003) 1745.
[10] P. van Espen, AXIL v3.0 Computer Code Manual, 1990.
[11] M.A. Reis, L.C. Alves, Nucl. Instrum. Methods B 68 (1992) 300.
[12] N.P. Barradas, C. Jeynes, R.P. Webb, Appl. Phys. Lett. 71 (1997) 291.
[13] V. Logvinenko, A. Minina, Yu. Mikhaylov, Yu. Yukhin, B. Bokhonov, J. Therm. Anal. Calorim. 74 (2003) 407.
[14] K. Asami, T. Osaka, T. Yamanobe, I. Koiwa, Surf. Interface Anal. 30 (2000) 391.
[15] K. Asami, I. Koiwa, T. Yamanobe, Jpn. J. Appl. Phys. 38 (2001) 5423.
[16] I. Rusu, M.-L. Craus, D. Sutiman, A. Rusu, J. Serb. Chem. Soc. 69 (2004) 53.
[17] E. Casado-Rivera, Z. Gál, A.C.D. Angelo, C. Lind, F.J. DisSalvo, H.D. Abruña, Chem. Phys. Chem. 4 (2003) 193.
[18] A.D. Li, D. Wu, H.-Q. Ling, T. Yu, Z.-G. Liu, N.B. Ming, Micorelectron. Eng. 66 (2003) 654.
[19] M.L. Calzada, A. González, J. García-López, R. Jiménez, Chem. Mater. 15 (2003) 4775.
[20] A. Asthagiri, D.S. Sholl, J. Chem. Phys. 116 (2002) 9914.
[21] B.-Y. Tsui, C.-F. Huang, IEEE Electron Dev. Lett. 24 (2003) 153.
[22] B.E. Watts, F. Leccabue, M. Fanciulli, G. Tallarida, Mater. Sci. Semicond. Process. 5 (2003) 147.
[23] J.F. Scott, Ferroelectric Memories, Springer Series in Advanced Microelectronics, 2000.